HEFAT2012
9th International Conference on Heat Transfer, Fluid Mechanics and Thermodynamics
16 – 18 July 2012
Malta

ON THE MERGING OF IMMERSED BOUNDARY AND PSEUDO-SPECTRAL FOURIER METHODOLOGIES FOR FLOWS WITH HEAT TRANSFER

Denise Kinoshita[1], Aristeu Silveira,Neto[1*], Felipe Mariano[2] and Leonardo Queiroz[1]
[1] Federal University of Uberlândia – Mechanical Engineering Faculty – Fluid Mechanical Laboratory
[2]Federal University of Goiás – School of Electric, Computational and Mechanical Engineering

*Author for correspondence
Department of Mechanical Engineering
Federal University of Uberlândia
Uberlândia, 38400-902 - Brazil
E-mail: aristeus@mecanica.ufu.br

ABSTRACT

A new numerical methodology combining Fourier pseudo-spectral and immersed boundary methods - IMERSPEC – has been developed for fluid flow problems modeled using the Navier-Stokes, mass and energy equations, for incompressible flows. The numerical algorithm consists in a Fourier pseudo-spectral methodology using the collocation method, where every kind of thermal boundary condition can be modeled using an immersed boundary method (Multi Direct Forcing Method). The IMERSPEC methodology was presented by [7]. The formulation for first (Dirichlet), second (Neumann) and third (Robin) kind of boundary condition for energy equation were developed and verified. Preliminary results are presented in the present paper.

INTRODUCTION

In the last two decades a lot of effort has been spent by the fluid dynamic scientific community to address two crucial but conflicting key issues in the science of computational fluid dynamics (CFD). These are associated with the need to model increasingly complex boundary conditions in one hand, and, at the same time, requiring high accuracy [1]. The great majority of engineering and geophysical fluid flow problems are characterized by very complex geometries that arise mainly from the irregular domain frontiers. This is often associated with the presence of moving and deformable geometries.

The methods used to solve flow problems over complex and moving geometries require moving and deforming meshes or even remaking the mesh after a given number of time steps. These procedures cause the methodologies to have a high computational cost and have a more complex implementation [2].

There are several methodologies to impose boundary conditions. A lot of works were carried out on volume penalization method, [18], [19], [20] and [21], some of them was used with the Fourier pseudo-spectral method [20] and [21], but in the present paper the immersed boundary methodology was used to impose the boundary conditions.

The immersed boundary methodology has been developed since 1970 by several researchers [3, 4, 5, 6]. This method reach a portion of the requirements described above; specifically, it can handle complex and moving geometries, using Cartesian mesh.

This methodology was applied by [7] to solve the flow over a driven cavity and over a backward facing step. The cavity flow was also simulated by [17], using a Chebyshev collocation method. This work was developed and applied for isothermal flows. Flows with heat transfer effects was simulated using immersed boundary methodology for boundary conditions of first, second and third type by [8], [9], [10], [11] and [12].

In special [10] used the multi-direct forcing scheme to ensure the temperature Dirichlet boundary conditions at the immersed boundary and the finite difference scheme was applied to solve heat transfer problems, the results showed second-order spatial accuracy when applied to solve the Taylor-Green vortices.

An accurate Navier-Stokes equations solver allows to obtain a better solution of a given flow problem in a given grid, as compared with a less accurate numerical method. In terms of high order accuracy, the family of the so called spectral methods [13] has been virtually unsurpassed. Spectral methods are characterized by exponential convergence to the exact solution with increasing grid size.

Within the family of spectral methods, the classical Fourier pseudo-spectral collocation method is probably the most impressive, due to its extremely high accuracy and its low

computational cost. Moreover, the pressure terms in the Navier-Stokes equations can be lumped together with the non-linear term, for incompressible flows. So, the Fourier pseudo-spectral collocation method does not requires the solution of a pressure Poisson equation. It results in an unusually fast time stepping procedure. These classical methods, however, are in general not applicable for over complex geometries. The Fourier collocation method, in particular, can only be used in flows with periodic boundary conditions.

The goal of the present work is to show a new methodology for incompressible flows with heat transfer and with three kinds of boundary conditions. It has been looked to combine the accuracy and low computational cost of the classical Fourier pseudo-spectral method [13] with flexibility in handling complex geometries allowed by the immersed boundary methods. Was introduced, specifically, the *IMERSPEC* method [7], which combines a classical Fourier pseudo-spectral method, with an immersed boundary method. The main goal is to take into account the effects arising from the presence of complex boundaries. Also, any spatial derivative is computed with spectral accuracy. In the present paper, a new model for boundaries conditions of first (Dirichlet), second (Newman) and third (Robin) types were developed, implemented and verified, using synthesized solutions for the Navier-Stokes and energy equations.

NOMENCLATURE

C_P	[kJ/kgK]	Heat capacity
dA	[m^2]	Area
$\vec{f}$	[N/m^3]	Forcing source term for the N-S equations at the domain Ω
$\vec{F}$	[N/m^3]	Forcing source term for the N-S equations at the domain Γ
$\vec{f}_T$	[N/m^3]	Forcing source term for energy equation at the domain Ω
$\vec{F}_T$	[N/m^3]	Forcing source term for energy equation at the domain Γ
$\vec{f}_{ss}$	[N/m^3]	Source term to a synthetized solutions for Navier-Stokes equation
$\vec{f}_{T_{SS}}$	[N/m^3]	Source term to a synthetized solutions for energy equations
$\vec{f}_{T_{IB}}$	[N/m^3]	Source term to a Immersed Boundary for energy equations at the domain Ω
h	[-]	Mesh size
L_r	[m]	Characteristic length
$\vec{n}$	[-]	Normal vector
N_x, N_y	[-]	Total mesh points in x and y direction
p	[kgPa]	Pressure of fluid
$\vec{q}''$	[W/m^2]	Heat flux
$\overrightarrow{RHS}$	[N/m^3]	Right hand side of the N-S equations
RHS_T	[N/m^3]	Right hand side of the energy equations
Re_{Lr}	[-]	Reynolds number
T	[K]	Flow temperature
t	[s]	Time
T_r	[K]	Maximum temperature
u	[m/s]	Velocity components in x direction
U_r	[m/s]	Maximum velocity
ϑ	[m/s]	Velocity components in y direction
$\vec{V}$	[m/s]	Velocity of fluid
$\vec{x}$	[m]	Particle position at the Ω domain
$\vec{X}$	[m]	Particle position at the Γ domain

Special characters

a	[-]	Constant
b	[-]	Constant
$\vec{k}$	[m^{-1}]	Wave number vector
TF	[-]	Fourier transform

Greek letters

α	[m^2/s]	Diffusion coefficient of internal energy
δ	[-]	Dirac delta function
Δt	[s]	Time step
Γ	[-]	Lagrangian domain
i	[-]	Imaginary number
κ	[W/mK]	Thermal conductivity
μ	[kg/ms]	Dynamic viscosity of fluid
ν	[m^2/s]	Cinematic viscosity of fluid
ρ	[kg/m^3]	Fluid density
Ω	[-]	Whole computational domain
θ		Generic field

Subscript

∞	Environment
PhD	Physical domain
ref	Reference domain
T	Temperature

Superscripts

n	Present time level
$\wedge$	Fourier spectral space variable
$*$	Temporary variable
num	Numerical solution
an	Analytical solution

MATHEMATICAL MODELING

The presented methodology is based on the merging process of the immersed boundary method with a classical Fourier pseudo-spectral method. Was started writing the equations in physical space. Then, the pseudo-spectral and immersed boundary methods are described. Finally, models for several kinds of boundary conditions are presented.

The mathematical model for incompressible flows of Newtonian fluids, with heat transfer is established with the energy, the Navier-Stokes and mass equations. These equations present source terms that model the boundary conditions for momentum and heat transfer. These equations are presented below:

$$\vec{\nabla}\cdot\vec{V} = 0\,, \tag{1}$$

$$\rho\frac{\partial\vec{V}}{\partial t} = \overrightarrow{RHS} + \vec{f}\,, \tag{2}$$

$$\rho C_p\frac{\partial T}{\partial t} = RHS_T + f_T\,, \tag{3}$$

$$\overrightarrow{RHS} = -\rho\vec{\nabla}\cdot\left(\vec{V}\vec{V}\right) - \vec{\nabla}p + \mu\nabla^2\vec{V} + \vec{f}_{ss}\,, \tag{4}$$

$$RHS_T = -\vec{\nabla}\cdot\left(\vec{V}T\right) + \kappa\nabla^2 T + f_{Tss}\,, \tag{5}$$

where $\vec{f}(\vec{x},t)$ is the source term for Navier-Stokes equations and $f_T(\vec{x},t)$ is the term source for the energy equation respectively. The terms $\vec{f}_{ss}(\vec{x},t)$ and $f_{Tss}(\vec{x},t)$ are the source term related to the synthetized solutions for Navier-Stokes and energy equations. These source terms model the boundary conditions as well as others kind of physical effects.

The main goal of the present work is to present a new model for the IMERSPEC methodology [7] extended for flows with heat transfer effects. In the following topic the models for $\vec{f}(\vec{x},t)$ and $f_T(\vec{x},t)$ source terms are presented. Particularly, a model for the energy source term is proposed for the boundary conditions of first, second and third types.

1. Boundary condition for the Navier-Stokes equations

In the present paper, only the Dirichlet boundary condition is presented for fluid flows. This boundary condition is characterized by the no slipping physical condition. So, a reference velocity is defined as:

$$\vec{V}_{ref}\left(\vec{X},t\right) \equiv \vec{V}_{\Gamma}\left(\vec{X},t\right), \tag{6}$$

where $\vec{V}_{\Gamma}\left(\vec{X},t\right)$ is the velocity of a material particle placed at an immersed boundary described by $\vec{X}$. The vector $\vec{x}$ is the particle position at the domain Ω_{PhD} as illustrated by Figure 1. This boundary condition, Equation (6), is transformed in a source term $\vec{f}(\vec{x},t)$, as presented by [7]. The Equation (2) is discretized in time using a first order Euler method, only as illustration purpose:

$$\rho\frac{\vec{V}^{n+1}(\vec{x})-\vec{V}^{n}(\vec{x})}{\Delta t} = \overrightarrow{RHS}^{n}(\vec{x}) + \vec{f}^{n+1}(\vec{x}). \tag{7}$$

A guess velocity $\vec{V}^{*}(\vec{x},t)$ is added and subtracted to the Equation (7), which results:

$$\rho\frac{\vec{V}^{n+1}(\vec{x})-\vec{V}^{n}(\vec{x})}{\Delta t} + \rho\frac{\vec{V}^{*n+1}(\vec{x})-\vec{V}^{*n+1}(\vec{x})}{\Delta t} = \overrightarrow{RHS}^{n}(\vec{x}) + \vec{f}^{n+1}(\vec{x}). \tag{8}$$

Equation (8) can be decomposed in the following two equations:

$$\rho\frac{\vec{V}^{*n+1}(\vec{x})-\vec{V}^{n}(\vec{x})}{\Delta t} = \overrightarrow{RHS}^{n}(\vec{x}), \tag{9}$$

$$\vec{f}^{n+1}(\vec{x}) = \rho\frac{\vec{V}^{n+1}(\vec{x})-\vec{V}^{*n+1}(\vec{x})}{\Delta t}. \tag{10}$$

Equation (10), was written for a material particle placed at $\vec{x}$. It can also be written for a particle that is placed at $\vec{X}$, over the immersed boundary:

$$\vec{F}^{n+1}\left(\vec{X}\right) = \rho\frac{\vec{V}_{ref}^{n+1}\left(\vec{X}\right)-\vec{V}^{*n+1}\left(\vec{X}\right)}{\Delta t}, \tag{11}$$

where $\vec{V}_{ref}^{n+1}\left(\vec{X}\right)$ is given by the first type or Dirichlet boundary condition and $\vec{V}^{*n+1}\left(\vec{X}\right)$ is obtained by interpolation of $\vec{V}^{*}(\vec{x},t)$ which is calculated using Equation (9). So, since $\vec{F}^{n+1}\left(\vec{X}\right)$ is obtained, it is distributed to the neighbouring of the interface and an approximation of $\vec{f}(\vec{x},t)$ is recuperated:

$$\vec{f}(\vec{x},t) = \int_{\Gamma}\vec{F}\left(\vec{X},t\right)\delta\left(\vec{x}-\vec{X}\right)d\vec{X}. \tag{12}$$

Known the force $\vec{f}(\vec{x},t)$, the velocity $\vec{V}^{*n+1,it+1}(\vec{x})$ is updated using Equation (9), rewritten as follows:

$$\vec{V}^{*n+1,it+1}(\vec{x}) = \vec{V}^{*n+1,it}(\vec{x}) + \frac{\Delta t}{\rho}\vec{f}^{n+1}(\vec{x}). \tag{13}$$

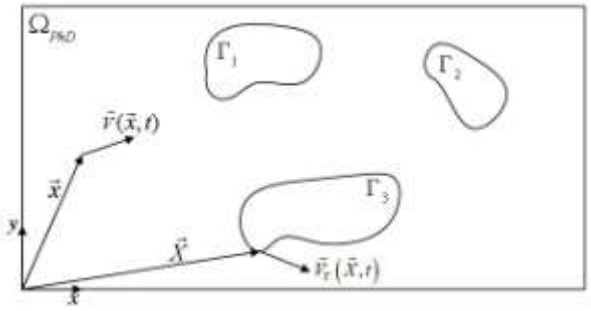

Figure 1 Illustration of the physical domain, Ω_{PhD}, and of the immersed boundaries Γ_i placed inside the physical domain.

2. Boundary conditions for the energy equation

Three kinds of boundary conditions will be proposed.

2.1. Dirichlet boundary condition (first type)

For this type of boundary condition the temperature $T(\vec{x},t)$ is given over the immersed boundary, which gives the reference temperature, defined as:

$$T_{ref}\left(\vec{X},t\right) \equiv T_{\Gamma}\left(\vec{X},t\right), \tag{14}$$

where $T_{ref}\left(\vec{X},t\right)$ is used in order to calculate the forcing term $f_T(\vec{x},t)$. In the present paper, this forcing term is calculated using the direct forcing, with a procedure similar to that used for the velocity. So, if we discretize Equation (3) using the

Euler time discretization method, as a guise of demonstration, we obtain:

$$\rho C_p \frac{T^{n+1}(\vec{x}) - T^n(\vec{x})}{\Delta t} = RHS_T^n(\vec{x}) + f_T^{n+1}(\vec{x}). \quad (15)$$

Adding and subtracting $T^{*n+1}(\vec{x})$ (guess of the temperature) on the left hand side of Equation (15), it gives:

$$\rho C_p \frac{T^{n+1}(\vec{x}) - T^n(\vec{x})}{\Delta t} + \rho C_p \frac{T^{*n+1}(\vec{x}) - T^{*n+1}(\vec{x})}{\Delta t} = RHS^n(\vec{x}) + f_T^{n+1}(\vec{x}). \quad (16)$$

This equation can be decomposed in the following two equations:

$$\rho C_p \frac{T^{*n+1}(\vec{x}) - T^n(\vec{x})}{\Delta t} = RHS_T^n(\vec{x}), \quad (17)$$

$$f_T^{n+1}(\vec{x}) = \rho C_p \frac{T^{n+1}(\vec{x}) - T^{*n+1}(\vec{x})}{\Delta t}. \quad (18)$$

Equation (18) can be rewritten for a material particle placed at the immersed boundary:

$$F_T^{n+1}(\vec{X}) = \rho C_p \frac{T^{n+1}(\vec{X}) - T^{*n+1}(\vec{X})}{\Delta t}, \quad (19)$$

where $T^{n+1}(\vec{X}) = T_{ref}^{n+1}(\vec{X})$ is given by the physical characteristic of each problem. On the other hand $T^{*n+1}(\vec{X},t)$ is obtained by the interpolation of $T^{*n+1}(\vec{x})$, which is given by the solution of Equation (17). This interpolation is given by the following equation:

$$T^{*n+1}(\vec{X}) = \int_{\Omega} T^{*n+1}(\vec{x})\delta(\vec{x} - \vec{X})d\vec{x}. \quad (20)$$

where $\vec{x} \in \Omega$ and $\vec{X} \in \Gamma$, as illustrated by Figure 1. Known $F_T^{n+1}(\vec{X})$, given by Equation (19), it can be distributed using the following equation:

$$f_T(\vec{x}) = \int_{\Gamma} F_T(\vec{X})\delta(\vec{x} - \vec{X})d\vec{X} = \int_{\Gamma} \rho C_p \frac{T^{n+1}(\vec{x}) - T^{*n+1}(\vec{x})}{\Delta t} d\vec{X}. \quad (21)$$

2.2. Newman boundary condition (second type)

For this type of boundary condition, the heat flux is given, or equivalently, the temperature gradient is known.

$$\vec{q}''(\vec{X},t) = -k_f \vec{\nabla} T(\vec{X},t). \quad (22)$$

We are looking to calculate $f_T^{n+1}(\vec{x})$ using the boundary condition given by Equation (22). Applying the gradient operator to Equation (18), it gives:

$$\vec{\nabla} f_T^{n+1}(\vec{x}) = \frac{\rho C_p}{\Delta t}\left(\vec{\nabla} T^{n+1}(\vec{x}) - \vec{\nabla} T^{*n+1}(\vec{x})\right). \quad (23)$$

This equation can be applied to a material particle that is placed beside an immersed boundary Γ:

$$\vec{\nabla} F_T^{n+1}(\vec{X}) = \frac{\rho C_p}{\Delta t}\left(\vec{\nabla} T^{n+1}(\vec{X}) - \vec{\nabla} T^{*n+1}(\vec{X})\right) = -\frac{\rho C_p}{\Delta t}\left(\frac{\vec{q}''^{n+1}(\vec{X})}{k_f} + \vec{\nabla} T^{*n+1}(\vec{X})\right). \quad (24)$$

The quantity $\frac{\vec{q}''^{n+1}(\vec{X})}{k_f}$ is given by the physical nature of the problem. On the other hand, $\vec{\nabla} T^{*n+1}(\vec{X})$ is obtained by the interpolation of $\vec{\nabla} T^{*n+1}(\vec{x},t)$ which is calculated after the solution of Equation (17):

$$\vec{\nabla} T^{*n+1}(\vec{X}) = \int_{\Omega} \vec{\nabla} T^{*n+1}(\vec{x})\delta(\vec{x} - \vec{X})d\vec{x}. \quad (25)$$

Equation (24) can be rewritten for a material particle placed at $\vec{x} \in \Omega_{PhD}$, given, approximately, by:

$$\vec{\nabla} f_T^{n+1}(\vec{x}) = \int_{\Gamma} \vec{\nabla} F_T^{n+1}(\vec{X})\delta(\vec{x} - \vec{X})d\vec{X} = \int_{\Gamma} \frac{\rho C_p}{\Delta t}\left(\frac{\vec{q}''^{n+1}(\vec{X})}{k_f} + \vec{\nabla} T^{*n+1}(\vec{X})\right)\delta(\vec{x} - \vec{X})d\vec{X}. \quad (26)$$

Applying the divergent operator to Equation (26), the following equation is obtained:

$$\nabla^2 f_T^{n+1}(\vec{x}) = \vec{\nabla} \cdot \underbrace{\int_{\Gamma} \frac{\rho C_p}{\Delta t}\left(\frac{\vec{q}''^{n+1}(\vec{X})}{k_f} + \vec{\nabla} T^{*n+1}(\vec{X})\right)\delta(\vec{x} - \vec{X})d\vec{X}}_{\vec{I}^{n+1}(\vec{x})} = \vec{\nabla} \cdot \vec{I}^{n+1}(\vec{x}). \quad (27)$$

There are many methods to solve Equation (27). Particularly, it is possible to solve this equation using the Fourier spectral method. It is possible even for non-periodical problems, as shown by [7]. Transforming this equation to the Fourier space, it gives:

$$\hat{f}_T^{n+1}\left(\vec{k},t\right)=-\frac{1}{k^2}TF\left\{\vec{\nabla}\cdot\vec{I}^{\,n+1}\left(\vec{x},t\right)\right\}. \tag{28}$$

So, from Equation (28), $\hat{f}_T^{n+1}\left(\vec{k}\right)$ or $f_T^{n+1}\left(\vec{x}\right)$, can be obtained and used to solve Equation (3).

2.3. Robin boundary condition (third type)

This is a hybrid boundary condition, which takes into account at the same time the temperature and its gradient at the immersed boundary. A differential equation can be obtained making an energy balance over the boundary. So, the heat flux given by diffusion in side of the boundary must be equals to the heat flux given by convection on the other side of the boundary, as illustrated by Figure 2. It gives the following equation:

$$-k_f\vec{\nabla}T\left(\vec{X},t\right)=h_f\left(T\left(\vec{X},t\right)-T_\infty\right)\vec{n}\left(\vec{X}\right)dA\left(\vec{X}\right), \tag{29}$$

which can be rewritten as follow:

$$\vec{\nabla}T\left(\vec{X},t\right)+\lambda T\left(\vec{X},t\right)\vec{n}\left(\vec{X}\right)=\lambda T_\infty\vec{n}\left(\vec{X}\right), \tag{30}$$

where $\lambda=\frac{h_f}{k_f}dA$. From Equation (18) we have:

$$\lambda\, f_T^{n+1}\left(\vec{x}\right)=\frac{\lambda\rho C_p}{\Delta t}\left(T^{n+1}\left(\vec{x}\right)-T^{*n+1}\left(\vec{x}\right)\right) \tag{31}$$

and

$$\vec{\nabla}f_T^{n+1}\left(\vec{x}\right)=\frac{\rho C_p}{\Delta t}\left(\vec{\nabla}T^{n+1}\left(\vec{x}\right)-\vec{\nabla}T^{*n+1}\left(\vec{x}\right)\right). \tag{32}$$

Equation (31) can be rewritten for a material particle placed at an immersed boundary. The resultant equation is still multiplied by the normal vector $\vec{n}$. This gives the following equation:

$$\lambda F_T^{n+1}\left(\vec{X},t\right)\vec{n}=\frac{\lambda\rho C_p}{\Delta t}\left(T^{n+1}\left(\vec{X},t\right)-T^{*n+1}\left(\vec{X},t\right)\right)\vec{n}\left(\vec{X},t\right). \tag{33}$$

Similarly, Equation (32) is rewritten at the immersed boundary, resulting:

$$\vec{\nabla}F_T^{n+1}\left(\vec{X}\right)=\frac{\rho C_p}{\Delta t}\left(\vec{\nabla}T^{n+1}\left(\vec{X}\right)-\vec{\nabla}T^{*n+1}\left(\vec{X}\right)\right). \tag{34}$$

Adding Equation (33) and (34), results:

$$\vec{\nabla}F_T^{n+1}\left(\vec{X}\right)+\lambda F_T^{n}\left(\vec{X}\right)\vec{n}=\frac{\rho C_p}{\Delta t}\left[\begin{array}{l}\left(\vec{\nabla}T^{n+1}\left(\vec{X}\right)-\vec{\nabla}T^{*n+1}\left(\vec{X}\right)\right)+\\ \lambda\left(T^{n+1}\left(\vec{X}\right)-T^{*n+1}\left(\vec{X}\right)\right)\vec{n}\left(\vec{X}\right)\end{array}\right]. \tag{35}$$

Equation (35) can be rewritten in a convenient form:

$$\vec{\nabla}F_T^{n+1}\left(\vec{X}\right)+\lambda F_T^{n+1}\left(\vec{X}\right)\vec{n}=\frac{1}{\Delta t}\left[\begin{array}{l}\underbrace{\left(\rho C_p\vec{\nabla}T^{n+1}\left(\vec{X}\right)+\lambda\rho C_pT^{n+1}\left(\vec{X}\right)\vec{n}\left(\vec{X}\right)\right)}_{=\lambda\rho C_pT_\infty\vec{n}}-\\ \left(\rho C_p\vec{\nabla}T^{*n+1}\left(\vec{X}\right)+\lambda\rho C_pT^{*n+1}\left(\vec{X}\right)\vec{n}\left(\vec{X}\right)\right)\end{array}\right]. \tag{36}$$

So, using Equation (30), it gives:

$$\vec{\nabla}F_T^{n+1}\left(\vec{X}\right)+\lambda F_T^{n+1}\left(\vec{X}\right)\vec{n}\left(\vec{X}\right)=\frac{1}{\Delta t}\left[\lambda\rho C_pT_\infty\vec{n}\left(\vec{X}\right)-\left(\begin{array}{l}\rho C_p\vec{\nabla}T^{*n+1}\left(\vec{X}\right)+\\ \lambda\rho C_pT^{*n+1}\left(\vec{X}\right)\vec{n}\left(\vec{X}\right)\end{array}\right)\right]. \tag{37}$$

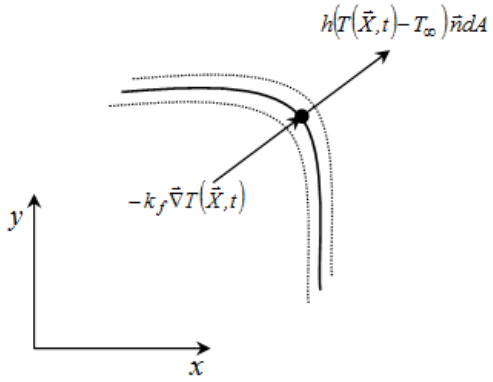

Figure 2 Balance of energy over an immersed interface.

Equation (37) can be formally rewritten in the Ω domain, giving approximately:

$$\vec{\nabla}f_T^{n+1}\left(\vec{x}\right)+\lambda\int_\Gamma F_T^{n+1}\left(\vec{X}\right)\vec{n}\left(\vec{X}\right)\delta\left(\vec{x}-\vec{X}\right)d\vec{X}=\frac{1}{\Delta t}\int_\Gamma\left[\begin{array}{l}\lambda\rho C_pT_\infty\vec{n}\left(\vec{X}\right)-\\ \left(\begin{array}{l}\rho C_p\vec{\nabla}T^{*n+1}\left(\vec{X}\right)+\\ \lambda\rho C_pT^{*n+1}\left(\vec{X}\right)\vec{n}\left(\vec{X}\right)\end{array}\right)\end{array}\right]\delta\left(\vec{x}-\vec{X}\right)d\vec{X}. \tag{38}$$

Applying the divergent operator to Equation (38), it gives:

$$\nabla^2 f_T^{n+1}\left(\vec{x}\right)+\vec{\nabla}\cdot\vec{I}_1^{n+1}\left(\vec{x}\right)=\vec{\nabla}\cdot\vec{I}_2^{n+1}\left(\vec{x}\right), \tag{39}$$

where

$$\vec{I}_1^{n+1}\left(\vec{x}\right)=\lambda\int_\Gamma F_T^{n+1}\left(\vec{X}\right)\vec{n}\left(\vec{X}\right)\delta\left(\vec{x}-\vec{X}\right)d\vec{X}\,, \tag{40}$$

and

$$I_2^{n+1}\left(\vec{x}\right)=\frac{1}{\Delta t}\int_\Gamma\left[\begin{array}{l}\lambda\rho C_pT_\infty\vec{n}\left(\vec{X}\right)-\\ \left(\begin{array}{l}\rho C_p\vec{\nabla}T^{*n+1}\left(\vec{X}\right)+\\ \lambda\rho C_pT^{*n+1}\left(\vec{X}\right)\vec{n}\left(\vec{X}\right)\end{array}\right)\end{array}\right]\delta\left(\vec{x}-\vec{X}\right)d\vec{X}. \tag{41}$$

Equation (39) can be solved by several methods. Particularly it is possible to be solved using a Fourier spectral method. In this case the periodical boundary condition must be used, as commented before. Applying the Fourier transform to Equation (39), it gives:

$$-k^2 \hat{f}_T^{n+1}(\vec{k}) + \vec{k} \cdot \hat{\vec{I}}_1^{n+1}(\vec{k}) = \vec{k} \cdot \hat{\vec{I}}_2^{n+1}(\vec{k}), \qquad (42)$$

from which the following equation is obtained:

$$\hat{f}_T^{n+1}(\vec{k}) = \frac{1}{k^2}\left[\vec{k} \cdot \hat{\vec{I}}_1^{n+1}(\vec{k}) - \vec{k} \cdot \hat{\vec{I}}_2^{n+1}(\vec{k})\right]. \qquad (43)$$

The solution of Equation (39) requires the integral $\vec{I}_1^{n+1}(\vec{x})$, which requires $F_T^{n+1}(\vec{X})$. So it must be explicitly given and $F_T^{n+1}(\vec{X})$ is replaced by $F_T^n(\vec{X})$.

3. Mathematical model in the Fourier spectral space

Given the mathematical model in the physical space, the next step is to transform it to the Fourier spectral space. For instance, the Fourier transform of the continuity equation gives:

$$i\vec{k} \cdot \hat{\vec{V}}(\vec{k},t) = 0, \qquad (44)$$

where $\hat{\vec{V}}(\vec{k},t)$ stands for the Fourier transform of the velocity field $\vec{V}(\vec{x},t)$. Equation (44) shows that the transformed velocity field is orthogonal to the wave number vector. The transformation of Equation (9) gives the estimated velocity $\vec{V}^*(\vec{x},t)$:

$$\rho \frac{\partial \vec{V}^*(\vec{x},t)}{\partial t} = -\mu k^2 \vec{V}^*(\vec{k},t) + \overline{\overline{\wp}} \cdot \left\{ \int_{\vec{k}=\vec{p}+\vec{q}} \vec{V}^*(\vec{p},t)\vec{V}^*(\vec{k}-\vec{p},t)\,d\vec{p} + \hat{\vec{f}}_{ss}(\vec{k},t) \right\}, \qquad (45)$$

where $\overline{\overline{\wp}}$ is the projection tensor presented by [13].

The transformation of Equation (17), gives the following equation:

$$\rho C_p \frac{\partial \hat{T}^*(\vec{k},t)}{\partial t} = -k^2 \hat{T}^*(\vec{k},t) + \vec{k} \cdot \int_{k=p+q} \hat{T}^*(\vec{p},t)\hat{\vec{V}}(\vec{k}-\vec{p},t)\,d\vec{p} + \hat{f}_{T_{SS}}(\vec{k},t). \qquad (46)$$

The non linear terms that appear at the right hand side of Equation (46) is given by the convolution integral, which is very expensive to be solved. Otherwise, they can be solved using the pseudo-spectral method, presented by [13]. It consists to make the product in the physical space and then transformed it to the Fourier spectral space. The *FFT (Fast Fourier Transform)* numerical algorithm, implemented by [16], is being used. It is worth to be emphasized that the pressure was eliminated from Navier-Stokes equations as can be seen in Equation (45). Nevertheless the pressure can be recuperated from the calculated velocity field, as shown by [7]. Note that this is only a pos-processing procedure.

4. The IMERSPEC methodology

The proposed algorithm is shortly presented by the next steps:

1. Solve Equation (45), using a low dispersion and low storage Runge-Kutta method proposed by [13], in order to obtain $\hat{\vec{V}}^*(\vec{k},t)$.

2. Use an inverse Fourier transform in order to obtain $\vec{V}^*(\vec{x},t)$.

3. Interpolate $\vec{V}^*(\vec{x},t)$ to obtain $\vec{V}^*(\vec{X},t)$ and then calculate $\vec{F}(\vec{X},t)$.

4. Make the distribution of $\vec{F}(\vec{X},t)$ in order to obtain $\vec{f}(\vec{x},t)$.

5. Update the velocity field $\vec{V}^*(\vec{x},t)$ and return to step (3).

The multi-forcing process, from step (3) to the step (5), is done up to a given maximum value of the L_2 norm is attained. Note that this norm measures how good is the model for the boundary condition, which is virtually imposed over the immersed boundary by the multi-forcing process.

6. Solve Equation (46) to obtain $\hat{T}^*(\vec{k},t)$. Perform the inverse Fourier transform to obtain $T^*(\vec{x},t)$.

7. Calculate $F_T(\vec{X},t)$ and after obtain $f_T(\vec{x},t)$.

8. Update the temperature field to obtain $T(\vec{x},t)$.

5. Synthesized solution for Navier-Stokes and energy equations

A synthesized or manufactured solution consists to determine a source term, given an analytical solution to the velocity, temperature and pressure field. The following equations, proposed by Green-Taylor [15], and a similar analytical solution for the energy equation, Equation (3), were used in the present work:

$$u^{an}(\vec{x},t) = U_r \sin\left(\frac{ax}{L_r}\right)\cos\left(\frac{by}{L_r}\right) e^{-\frac{\nu t}{L_r^2}\left(a^2+b^2\right)}, \qquad (46)$$

$$\vartheta^{an}(\vec{x},t) = -U_r \frac{a}{b}\cos\left(\frac{ax}{L_r}\right)\sin\left(\frac{by}{L_r}\right) e^{-\frac{\nu t}{L_r^2}\left(a^2+b^2\right)} \qquad (47)$$

$$p^{an}(\vec{x},t) = -\rho U_r^2 \frac{a^2}{2b^2}\left[\cos\left(\frac{by}{L_r}\right)^2 - \sin\left(\frac{by}{L_r}\right)^2\right] e^{-2\frac{\nu t}{L_r^2}\left(a^2+b^2\right)}$$

, (48)

$$T^{an}(\vec{x},t) = T_r \sin\left(\frac{ax}{L_r}\right)\cos\left(\frac{by}{L_r}\right)\cos\left(\frac{\alpha t}{L_r^2}\right), \quad (49)$$

where, u^{an}, ϑ^{an}, p^{an} and T^{an} are, respectively, the analytical solution for the velocity components, the pressure and the temperature. The terms *a* and *b* are constants, L_r is a characteristic length, α is the diffusion coefficient of internal energy, *x* and *y* are the components of the coordinates system, *t* is the time, ρ and ν are the fluid density and the cinematic viscosity respectively. It should be observed that when *u*, ϑ and *p* in Equation (2) (Navier-Stokes equations) are replaced by Equations (46), (47) and (48), results in a source term $\vec{f}_{ss}(\vec{x},t) = \vec{0}$. This is the main characteristic of the Green-Taylor analytical solution. The source term $f_{Tss}(\vec{x},t)$, due to the synthetized solution for the energy equation is obtained replacing Equation (46), (47) and (49) at Equation (3) results:

$$f_{T_{SS}}(\vec{x},t) = \frac{\rho C_p T_r}{L_r^2}\sin\left(\frac{ax}{L_r}\right)\left[\begin{array}{l}\alpha\cos\left(\frac{by}{L_r}\right)\cos\left(\frac{\alpha t}{L_r^2}\right)+ \\ U_r a L_r \cos\left(\frac{ax}{L_r}\right)e^{-\frac{\nu t}{L_r^2}(a^2+b^2)}\sin\left(\frac{\alpha t}{L_r^2}\right)+ \\ \alpha a^2\cos\left(\frac{by}{L_r}\right)\sin\left(\frac{\alpha t}{L_r^2}\right)+ \\ \alpha b^2\cos\left(\frac{by}{L_r}\right)\sin\left(\frac{\alpha t}{L_r^2}\right)\end{array}\right]. \quad (50)$$

In order to compare the numerical simulation with analytical solution, the initial and boundary conditions were determined using this analytical solution. This procedure results in periodical boundary conditions, which is appropriated as a reference for the Fourier pseudo-spectral method.

The control parameters, as suggested by [7], are: the diameter of vortices, $L_r = \pi$ [m], the maximum velocity $U_r = \max\left[u^{an}(t=0), \vartheta^{an}(t=0)\right]$ which is chosen as 1 [*m/s*]. The reference time is given by $\frac{L_r}{U_r} = \pi$ [*s*]. The Reynolds number is defined by the following equation:

$$Re_{Lr} = \frac{U_r L_r}{\nu}. \quad (51)$$

As the viscosity is taken equals to 1, the Reynolds number assumes also the value 1. The dimensionless constants *a*=1 and *b*=1 was taken.

The main goal of this simulation is to perform the verification of the proposed methodology and its numerical implementation. For that, the velocity and temperature fields were obtained numerically. The pressure field was recuperated as a post-processing procedure, as shown by [7]. Then, the velocities components, the temperature and the pressure fields were compared with the analytical solution (Equations (46), (47), (48) and (49)) and the norm L_2 was obtained using the following equation:

$$L_{2\theta} = \sqrt{\frac{\sum_i^{N_x}\sum_j^{N_x}\left(\theta_{ij}^{num} - \theta_{ij}^{an}\right)^2}{N_x N_y}}, \quad (52)$$

where θ^{num} and θ^{an} stand, respectively, for the numerical and the analytical solution of the generic field, θ, *i.e.*, u, ϑ, p and T. The global error of the simulation can be determined using the norm L_2, calculated over the entire domain at each time. The solution and the domain present a periodical behavior. In order to use the boundaries conditions, modeled by the immersed boundary methodology, it is possible to insert, inside this domain, an immersed boundary over which all kind of boundary condition can be modeled and simulated using the forcing method.

RESULTS

1. The Green Taylor problem with thermal effects, without immersed boundary

The first case that was simulated and used to verify the numerical pseudo-spectral code was the Green-Taylor problem, with thermal effects. So, Equation (45) and (46) were solved, using the pseudo-spectral method, considering the immersed boundary source terms $\hat{\vec{f}}(\vec{k},t) = \vec{0}$ and $\hat{f}_{T_{SS}}(\vec{k},t)$. The term $\hat{f}_{T_{SS}}(\vec{k},t)$ is given by Equation (50). The boundary and initial conditions are given by the analytical solutions. Figure 3 shows the velocity, the pressure and the temperature field. All them are periodical. The errors between the numerical solution (pseudo-spectral method) and the analytical solution for velocity, pressure and temperature were obtained using the Equation (52) and they are shown at Figure 4.

2. The Green Taylor problem with thermal effects, with immersed boundary

This case is characterized by the presence of an immersed boundary Γ inside the complete domain Ω; a continuous initial condition is given by Equation (49); the thermal source term $f_{T_{SS}}(\vec{x},t)$, for the synthesised solution is given by Equation (50).

The source term $\hat{f}_{T_{IB}}(\vec{k},t)$, for the proposed immersed boundary method, is given by the first type boundary condition (Dirichlet), Equation (18), by the second type boundary condition (Newman), Equation (28) and by the third type boundary condition (Robin), Equation (43).

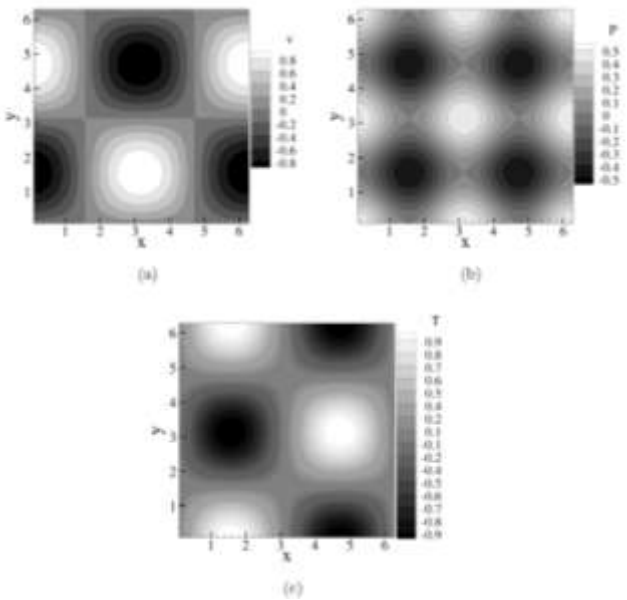

Figure 3 The Green-Taylor vortices; N_xxN_y=64x64 collocations nodes: (a) the horizontal velocity component (v); (b) pressure (p) and (c) temperature (T).

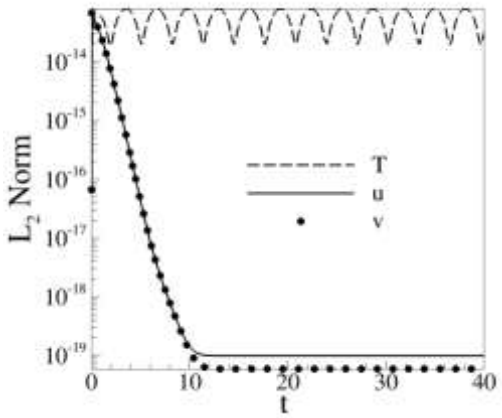

(a)

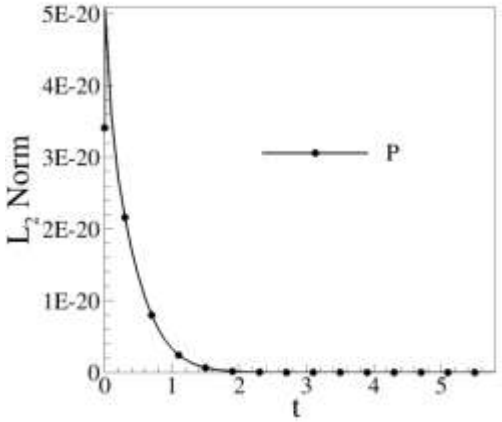

(b)

Figure 4 The errors (L_2) for the Green-Taylor N_xxN_y=64x64 collocations nodes: (a) velocities and temperature and (b) pressure.

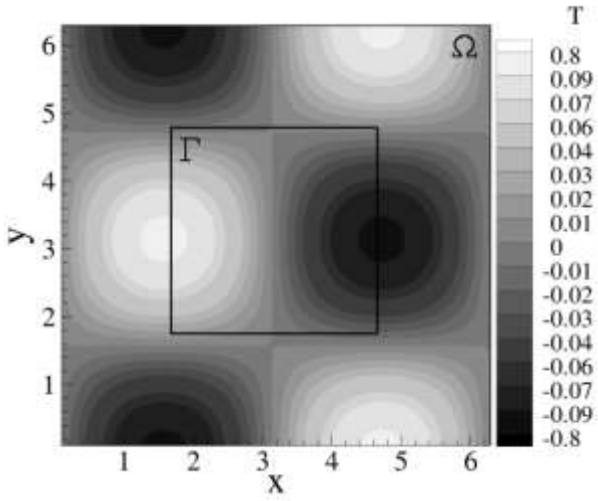

Figure 5 The temperature field; immersed boundary Γ inside the complete domain Ω.

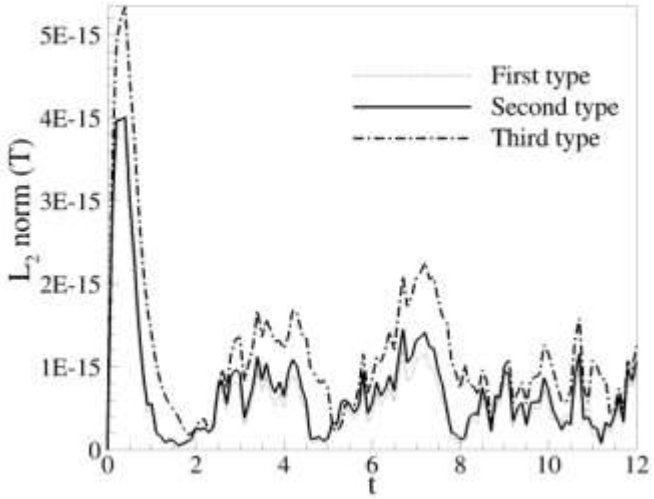

Figure 6 The errors (L_2) of the temperature for the Green-Taylor problem, with thermal effect and with immersed boundary; N_xxN_y=64x64 collocations nodes: first, second and third type thermal boundary condition.

Figure 5 shows the temperature field and the immersed boundary inside the global domain. The global error, given by Equation (52) is shown by Figure 6, for the boundary conditions of first, second and third type. It can be seen that the boundary conditions keep the accuracy of the spectral method when the immersed boundary methodology is used.

The rate of convergence was approximately 8 to the N_xxN_y=8x8, 16x16 and 32x32 collocations points. Above this resolution, it reaches round-off truncation error.

CONCLUSION

A new kind of immersed boundary methodology for fluids flows with thermal effects was proposed. Mathematical model for thermal boundary conditions of first, second and third types were proposed. They were implemented in a pseudo-spectral numerical code. The implementation was verified using a synthetized analytical solution for the Navier-Stokes and energy equations. The simulations that are presented in the present paper show that the proposed methodology is very accurate, at least for the simulated problem.

ACKNOWLEGMENTS: The authors would like to thanks to PETROBRAS, FAPEMIG, CAPES/PROEX, CNPq, UFU and UFGO for the support for the development of the present work.

REFERENCES

[1] Ferziger J.H., and Peric, M., Computational Methods for Fluid Dynamics, Springer, 1996.

[2] Nakahashi K., Ito Y., and Togashi F., Some challenges of realistic flow simulations by unstructured grid cfd, *International Journal for Numerical Methods in Fluids*, Vol. 43, 2003, pp. 769–783.

[3] Peskin C.S., Flow patterns around heart valves: a numerical method, Vol. 10, 1972, pp. 252–271.

[4] Goldstein D., Adachi T., and Sakata H., Modeling a no-slip flow with an external force field, *Journal of Computational Physics*, Vol. 105, 1993.

[5] Lima e Silva A.L., Silveira-Neto A., and Damasceno J., Numerical simulation of two dimensional flows over a circular cylinder using the immersed boundary method, *Journal of Computational Physics*, Vol. 189, 2003, pp. 351–370.

[6] Mittal R., and Iaccarino G., Immersed boundary methods, *Annual Review Fluid Mechanics*, Vol. 37, 2005, pp. 239–261.

[7] Mariano F.P., Moreira L.Q., Silveira-Neto A., Silva C.B., and Pereira J.C.F., A new incompressible navier-stokes solver combining Fourier pseudo-spectral and immersed boundary method, *Computer Modeling in Engineering Science*, Vol. 59, 2010, pp. 181–216.

[8] Jungwoo K., and Haecheon C., An Immersed-Boundary Finite-Volume Method for Simulation of Heat Transfer in Complex Geometries, *KSME International Journal*, Vol. 18, 2004, pp. 1026-1035.

[9] Jeong H.K., Yoon H.S., Ha M.Y., and Tsutahara M., An immersed boundary-thermal lattice Boltzmann method using an equilibrium internal energy density approach for the simulation of flows with heat transfer, *Journal of Computational Physics*, Vol. 229, 2010, pp. 2526–2543.

[10] Wang Z., Fan J., Luo K, and Cen K., Immersed boundary method for the simulation of flows with heat transfer, *International Journal of Heat and Mass Transfer*, Vol. 52, 2009, pp. 4510–4518.

[11] Pan D., An immersed boundary method on unstructured Cartesian meshes for incompressible flows with heat transfer, *Numerical Heat Transfer, Part B*, Vol. 49, 2006, 277–297.

[12] Young D.L., Jan Y.J., and Chiu C.L., A novel immersed boundary procedure for flow and heat simulations with moving boundary, *Computers & Fluids*, Vol. 38, 2009, pp. 1145–1159.

[13] Canuto C., Hussaini M.Y., Quarteroni A., and Zang T.A., Spectral methods: evolution to complex geometries and applications to fluid dynamics, Spriger Verlag, 2007.

[14] Allampalli V., Hixon R., and Nallasamy M., Sawyer, S., High-accuracy large step explicit runge - kutta (HALE-RK) schemes for computational aero acoustics, *Journal of Computational Physics*, Vol. 228, 2009, pp. 3837–3850.

[15] Taylor G.I., and Green A.E., Mechanism of production of small eddies from large ones. *Proceedings Royal Society London*, Vol. 158, 1937, pp. 49-521.

[16] Takahashi D., A hybrid MPI/OpenMP implementation of a parallel 3-D FFT on SMP clusters. *Lecture Notes in Computer Science*, Vol. 3911, 2006, pp. 970-977.

[17] Botella O., and Peyret R., Benchmark spectral results on the lid-driven cavity flow. *Computer & Fluids*, Vol. 27, 1998, pp. 421-433.

[18] Paccou A., Chiavassa G., Liandrat J., Schneider K., A penalization method applied to the wave equation. *Comptes Rendus Mecanique*, Vol. 333, 2005, pp. 79-85.

[19] Pasquetti R., Bwemba R., Cousin L., A pseudo-penalization method for high Reynolds number unsteady flows. *Applied Numerical Mathematics*, Vol. 58, 2008, pp. 946-954.

[20] Scheneider K., Farge M., Numerical simulation of the transient flow behaviour in tube bundles using a volume penalization method. *Journal of Fluids and Structures*, Vol. 20, 2005, pp. 555-566.

[21] Kolomenskiy D., Moffatt H.K., Farge M., Schneider K., Two- and three-dimensional numerical simulations of the clap –fling-sweep of hovering insects. *Journal of Fluids and Structures*, Vol. 27, 2011, pp. 784-791.